RESEARCH

Shared datasets for IMRT, beam angle optimization, and VMAT research

David Craft[1*], Mark Bangert[2], Troy Long[3], Dávid Papp[1] and Jan Unkelbach[1]

[*]Correspondence: dcraft@mgh.harvard.edu
[1]Massachusetts General Hospital, Harvard Medical School, Boston, MA
Full list of author information is available at the end of the article
[†]Equal contributor

Abstract

Background: We provide common datasets for researchers to use when developing and contrasting radiation treatment planning optimization algorithms. The datasets allow researchers to make one-to-one comparisons of algorithms to solve various instances of the radiation therapy treatment planning problem in intensity modulated radiation therapy (IMRT), including beam angle optimization (BAO), volumetric modulated arc therapy (VMAT) and direct aperture optimization (DAO).

Dataset: We provide datasets for a prostate case, a liver case, a head and neck case, and a standard IMRT phantom. For each, we provide the dose-influence matrix from a variety of beam/couch angle pairs. The dose-influence matrix is the main entity needed to perform optimizations: it contains the dose to each patient voxel from each pencil beam. We also provide the original DICOM computed tomography (CT) scan as well as the DICOM structure file.

Conclusions: We provide an open dataset – the first of its kind – to the radiation oncology community, which will allow researchers to compare methods for optimizing radiation dose delivery.

Keywords: IMRT; optimization; radiation therapy; beam angle optimization; VMAT; treatment plan optimization

Background

The goal of radiation therapy for cancer treatment is to irradiate the tumorous regions of the body with sufficiently high levels of radiation while sparing the nearby healthy tissues as much as possible. In the mid 1990s a technique known as intensity modulated radiation therapy (IMRT) emerged which allows for much more tailoring of the 3D dose distribution inside the patient. Along with this extra freedom comes the need for mathematical optimization, and over the last 20 years a large amount of research has produced over of 600 papers revolving around this topic (this is a conservative estimate based on a PubMed search for the words "IMRT" and "optimization" in the title or abstract).

A deficiency in the field has been the lack of common datasets for researchers to test their algorithms on. As such, most new algorithm papers simply state the algorithm and demonstrate it, but the reader is left to wonder how this algorithm compares with other approaches to the same problem. The raw data which was used for a specific study is never provided as part of the publication. Reasons include the data size, involvement of commercial software products, and protection of data privacy for individual patients.

With this paper, we want to address these issues and provide the basis for meaningful benchmarking of IMRT optimization algorithms. Specifically, our initiative aims at resolving the following shortcomings:

- Patient cases used in different papers differ greatly in the geometry of their targets and critical sturctures. A technique that works on an "easy" patient may not work as well on a "hard" patient and vice versa.
- Research papers make different assumptions when deriving plan optimization data from the patient's planning CT. This includes the dose calculation method, spatial resolution of the dose and beamlet grid, planning goals, delivery modality, etc. These data are generated in-house and are not shared with the research community.
- New researchers in the field may not have access to clinical patient datasets.

The datasets we present herein are applicable to IMRT [1, 2, 3] and its variants, including beam angle optimization (BAO) [4, 5, 6, 7], volumetric modulated arc therapy (VMAT) [8, 9, 10, 11, 12, 13], 3D-conformal optimization [14, 15], stereotactic body radiation therapy (SBRT) [16], and direct-aperture optimization (DAO) [17, 18, 19, 20, 21, 22]. We refer the readers to the citations for explanations of each of these (overlapping) modalities.

Data description

We provide datasets for three anonymized cancer patient cases and one standard IMRT phantom. For each of the four cases, we include the original DICOM CT image as well as the DICOM RTStruct file containing the contours of targets and organs at risk. These files are made available for viewing results, although they are not necessary for optimization. In addition, the DICOM files give researchers to opportunity to replan these patients in a commercial treatment planning system. All further data is derived from the DICOM data.

Voxel grid

For dose calculation, the original CT image is downsampled to a lower resolution. The final resolution and size of the dose grid in three dimensions is stored in a text file named CTVOXEL_INFO.txt. Each voxel in the 3D dose grid is assigned a voxel index, which is used in optimization data described below. The coordinate system and the conversion of voxel indices to spatial location is described in Appendix A. For standard optimizations, voxel positions are not needed. They are however needed for visualization of the dose distribution, and are useful for implementing objective functions which require spatial information, for example a dose penalty which depends on the distance from a normal tissue voxel to the patient's tumor. This file also contains the isocenter location. The isocenter is the common point that all the beams pass through.

Beamlet grid

The incident fluence is discretized into a rectangular grid of beamlets. We use a beamlet size of 1 cm by 1 cm for all cases except for the head and neck case, for which we use 0.5 cm by 0.5 cm. The isocenter is identical for all beam directions and is located in the center of mass of the union of all target volumes. The set of beamlets

for which dose is calculated is based on an isotropic 2.5 mm expansion of the union of all targets. A beamlet is included in the fluence map if its central axis intesects the enlarged target. In a post-processing step, we ensure that the beamlet grid is consecutive. If beamlets are missing from the fluence map, causing a hole across an MLC row, these beamlets are added and their dose distribution is calculated. This issue arises for example in the head and neck case with disconnected targets on either side of the neck. Missing beamlets could be problematic for sliding window IMRT and VMAT optimization approaches, where the MLC leaves would potentially slide over those beamlets. The beamlet grid coordinate system is described in Appendix A

Optimization data

All binary formatted data are saved from Matlab as *.mat files (we have used Matlab version 7.14.0.739, R2012a)[1]. In this way, data can either be read into Matlab, Octave, or Python using the scipy package. Instructions for reading in the data are given in the Methods section. For treatment plan optimization, we provide the following files for each patient.

Voxel lists

The voxel list files contain the voxel indices of the voxels which are inside each geometrically contoured structure. The information is stored as a list of integers in the files {structure name}_VOILIST.mat. The format thus allows for overlapping structures, i.e. a given voxel index can be contained in multiple voxel lists.

Beamlet information

For each (gantry angle, couch angle) pair, a beam info file with the file name Gantry{gantry angle}_Couch{couch angle}_BEAMINFO.mat is provided. The file contains the following information:

- couch angle
- gantry angle
- number of beamlets
- number of non-zeros in the dose-influence matrix (see next section; this value is helpful for pre-allocating memory to store these matrices)
- A vector of the x position of each of the beamlets (using the gantry head coordinate system, see figure 3).
- A vector of the y position of each of the beamlets (see figure 3).

Geometric beamlet information is not necessary for the most basic type of IMRT optimization, but for VMAT, and DAO (where "apertures" are created by combining adjacent beamlets), it is necessary to know the geometric location of each of the beamlets.

---

[1]Note that, if one were to use a more recent version of Matlab to save data for reading into Python etc, one should use the Matlab toggle -v7 during the save command.

Dose-influence matrix

The dose influence matrix D_{ij} is the main entity used for optimization. It contains the dose delivered to each voxel i per unit intensity of beamlet j. We provide the dose influence matrix in units of Gray per monitor unit (Gy/MU) [2]. The dose-influence matrix is stored in seperate files for each (gantry angle, couch angle) pair in files named Gantry{gantry angle}_Couch{couch angle}_D.mat. Each of these files contains a single matrix called D, which is a Matlab sparse matrix [3]. We use CERR version 4.4 (Computational Environment for Radiotherapy Research) [23] to produce the dose influence matrices for each case. CERR uses a pencil beam type dose calculation algorithm referred to as the quadrant infinite beam (QIB) model [24].

The dose to voxel i is given by $d_i = \sum_j D_{ij} x_j$ where x_j is the fluence value of the jth beamlet.

Hints for CERR users

To generate the optimization data, the dicom CT data was imported into CERR and the CT scan was then resampled to the voxel sizes shown in Table 1. This was done using the CERR command downSampleScan. Once the data was downsampled, the CERR IMRTP module was used to create the dose-influence matrices. Our group has modified this code to allow for couch rotations. The dose-influence matrix was then extracted from the internal CERR data structure and rescaled to units of Gy/MU. We also provide a Matlab .mat which is generated by CERR when saving the patient. This file contains, among other attributes, the downsampled CT scan, which has the same resolution as the dose grid, and can be used for visualization. For size purposes, this file does not contain the D_{ij} matrices.

The four cases

We provide data sets for four patients of different sizes to support a variety of radiotherapy planning problems and represent typical treatment sites. The main characteristics of all datasets are summarized in Table 1. A representative transversal slice through the CT, illustrating the geometry of target and OARs for each case, is shown in figure 1.

TG119 dataset

The first case we use is a phantom provided by the American Association of Physicists in Medicine Task Group 119 for use in institutional IMRT commissioning (i.e. readying a clinic for IMRT treatments) [25]. This phantom has several sets of contours for various IMRT treatment planning tests, but we only use three of the contours: a C-shaped target (called "OuterTarget"), an OAR that the target

[2] The unit of beamlet intensity (MU) is defined such that 100 MU yields a dose of 1 Gy in 10 cm depth in water in the center of a 10 cm by 10 cm radiation field.

[3] The dose influence matrix can by read directly into Matlab, Octave and Python as a sparse matrix (see the Methods section). Note however that Python is 0-based whereas Matlab and Octave are 1-based. The voxels indices stored in the {structure name}_VOILIST.mat files are 1-based, i.e., the lowest voxel index is 1, as depicted in figure 2. Thus the user has to perform the appropriate shift when using Python.

wraps around ("Core"), and the external contour of the phantom itself ("BODY"). For this case we provide five equispaced coplanar beams (coplanar refers to beams where the couch angle is fixed at 0°) at gantry angles 0°, 72°, 144°, 216°, and 288°. This serves as our small dataset. The total number of beamlets at each respective angle is 98, 70, 90, 90 and 70, for a total of 418 beamlets.

	TG119	Prostate	Liver	Head and neck
Number of beam angles	5	180	56	1983
Total number of beamlets	418	25,404	3678	2,257,507
Noncoplanar	no	no	yes	yes
Beamlet size [cm]	1x1	1x1	1x1	0.5x0.5
Voxel resolution (LR,AP,SI) [mm]	(3.0, 3.0, 2.5)	(3.0, 3.0, 3.0)	(3.0, 3.0, 2.5)	(3.0, 3.0, 5.0)
Voxel grid size (LR,AP,SI)	(167,167,129)	(184,184,90)	(217, 217,168)	(160,160,167)
Number of target voxels	7429	9491	6954	25,388
Number of voxels in patient	599,440	690,373	1,927,357	251,893
dataset size	25 MB	1.9 GB	560 MB	64 GB

Table 1: Summary of Patient characteristics. Number of target voxels for the head and neck case is for the union of the three PTV structures.

Prostate

The prostate case serves as one of our two medium size datasets. We generate 180 equispaced coplanar beams, thus this data set serves as a test case for VMAT algorithms. Using a beamlet resolution of 1cm×1cm, the total number of beamlets is 25,404. There are two targets for the prostate case. The highest prescription dose target, PTV_68, is a geometric expansion of the prostate. The lower dose target, PTV_56, is an expansion around the prostate and the lymph nodes.

SBRT liver case

This is the first non-coplanar case we present. We originally generate 162 (gantry, couch) angle pairs such that the entry angles are evenly scattered over a sphere corresponding to an average angular spacing of 16°. This was done using a Matlab routine called GridSphere available from the File Exchange portion of the MathWorks website. We then eliminate beams that have either entrance or exit doses through the first slice of the CT since if this is the case, the full dose deposit of the beam is not properly accounted for. This leaves 56 beams in the dataset, with a total of 3678. Note that given a particular linac, some gantry/counch angle combinations may not be allowed due to mechanical collisions. Since this is linac specific, we have not attempted to eliminate such beams, and instead leave it to the reader to keep this in mind if modeling an actual clinical delivery situation.

Head and neck

This serves as our large dataset. The CT and structures are obtained from the publically available research set www.cancerimagingarchive.net. This set was created with non-coplanar VMAT in mind and creates a full set of equispaced beams for a variety of couch angles. The couch angles are -90° to 90° in increments of 5°. At the couch angles -90, 0, and 90, we place beams at a 2° gantry spacing. At the other couch angles we use a 5° gantry spacing. 2° resolution is the clinical standard gantry discretization for computing VMAT doses; 5° is adequate for research purposes. We eliminate beams that enter through the inferior most CT slice, where the CT scan

ends. The elimination map is shown in Figure 4. This leaves 1983 beam angles used, with a total of 2,257,507 beamlets. The beamlets for this case are 0.5cm×0.5cm. the voxel resolution is 3mm×3mm×5mm. Unfortunately we cannot provide data at a higher resolution in the sup-inf direction due the sparse resolution of 5mm in the original CT. Still, this is perfectly adequate for computation research purposes.

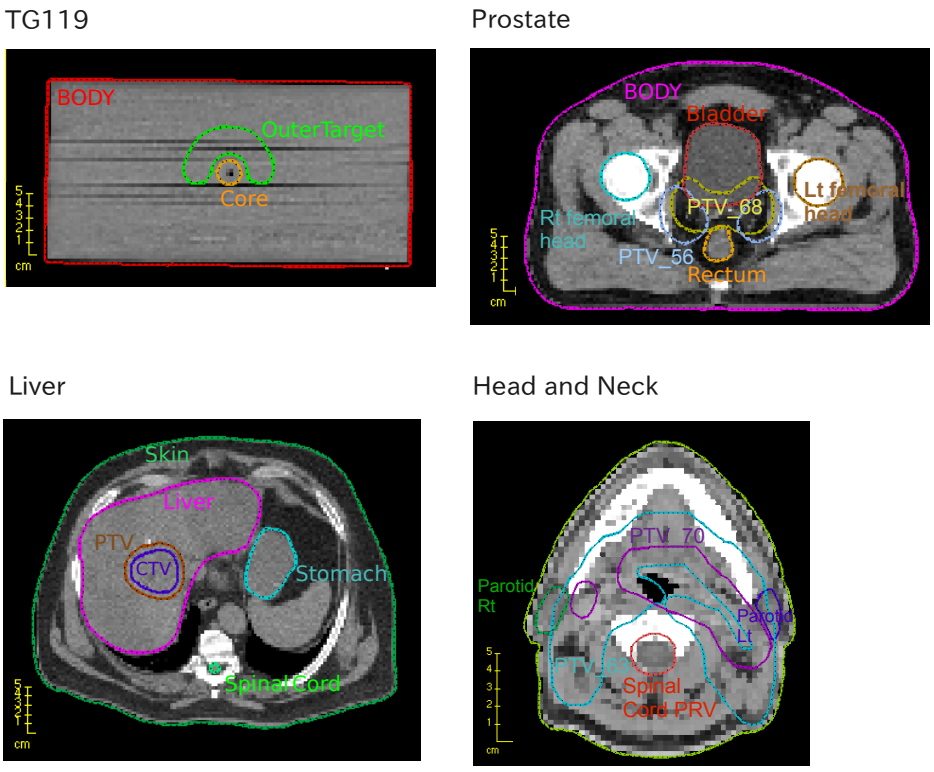

Figure 1 Axial views of the four cases CT and structures for the four cases for a representative CT slice (which shows some but not all of the structures included in the dataset).

Analyses

As a data verification step, we give dose distribution statistics for the ones solutions ($x_j = 1$ for all j) for all cases. We give the dose statistics for two volumes from each case, one target and one critical structure, see Table 2. In the Methods section we provide the Matlab code used to perform this calculation.

Case	Structure name	minimum dose	mean dose	maximum dose
TG119	Core	0.026798	0.050724	0.053313
	OuterTarget	0.049379	0.051067	0.052702
Prostate	PTV_56	1.3015	1.3631	1.4089
	Bladder	0.66549	1.2753	1.3863
Liver	Heart	0.0003963	0.093117	0.4388
	PTV	0.37532	0.41629	0.48094
Head and Neck	PTV_70	19.5394	21.0998	23.1338
	PAROTID_LT	8.7997	20.3354	23.7127

Table 2: Dose statistics for all cases, for two selected structures, for the ones solution (all beams), i.e. $d_i = \sum_j Dij$. This serves as a data consistency check for users.

Optimization demonstration and results

Description of the IMRT optimization problem

Here we describe what is known as the fluence-based IMRT optimization problem. This an idealized version of the actual IMRT treatment planning problem, but is commonly used to develop algorithms and indeed is possible to use in clinical settings (e.g. [26]).

For a set of beams, we assume the D matrix represents the entire set of beamlets from all the beams. That is, below D is interpreted as a concatenation of the individual D matrices from each beam. This notationally simplifies the problem, allowing us to avoid looping over the beams, instead we just loop over all beamlets. Let d be the vector of voxel doses, and let x be the vector of beamlet fluences. The key mapping is the linear relationship between the beamlet vector and the dose distribution and is given by $d = Dx$, where matrix-vector multiplication is used as shorthand for $d_i = \sum_j D_{ij} x_j$. Writing this dose calculation in the form of a matrix-vector product, a generic formulation of the IMRT optimization prolem is as follows:

$$\begin{aligned} \text{minimize} \quad & f(d) \\ & Dx = d \\ & d \in C \\ & x \geq 0, \end{aligned} \tag{1}$$

A specific example that would give rise to a linear program would be to choose as $f(d)$ the mean dose to a critical structure, and to invoke upper bounds for all voxels and additional lower bounds for the target voxels via the constraint set C. A typical quadratic formulation would set goals for every voxel (for example, prescription dose to all target voxels and 0 to all other voxels) and minimize the squared deviation from those levels.

BAO, DAO, and VMAT formulations put additional restrictions on the x vector. For example for BAO, one might restrict that a total of 5 beams are used at most, and thus integer variables could be added to this formulation to control the maximum number of active beams/beamlets.

Examples of linear programming formulations

Here we present simple linear programming formulations and summary results for each of the four cases. These formulations are not meant to produce quality treatment plans but are rather selected to be simple to implement and thus reproduce results as a baseline.

Objective	min (mean Core + mean BODY)
Constraints	OuterTarget >= 1
	OuterTarget <=1.2
	Core <=1.2
Results	mean Core = 0.2489
	mean BODY = 0.1021

Table 3: Linear programming formulation and solution statistics for the TG119 case, all five beams used.

Objective	min (mean Rectum + 0.6*mean Bladder+ 0.6*mean BODY)
Constraints	PTV_68 >= 1
	x <=50
Results	mean Rectum = 0.2842
	mean Bladder = 0.4035
	mean BODY = 0.0905

Table 4: Linear programming formulation and solution statistics for the Prostate case, using the five beams at gantry angles 0°, 72°, 144°, 216°, and 288°.

Objective	min (mean Liver + mean Heart+ 0.6*mean entrance)
Constraints	PTV >= 1
	x <=25
Results	mean Liver = 0.1771
	mean Heart = 0.1258
	mean Entrance = 0.0186

Table 5: Linear programming formulation and solution statistics for the Liver case, using the seven beams at (gantry, couch) angles (58°, 0°), (106°, 0°), (212°, 0°), (328°, 0°), (216°, 32°), (226°, -13°), (296°, 17°).

Objective	min (mean Left Parotid + mean Right Parotid
Constraints	All PTVs >= 1
	spinal cord <=0.5
	brainstem <=0.5
	x <=25
Results	mean Left Parotid = 0.4959
	mean Right Parotid = 0.3437

Table 6: Linear programming formulation and solution statistics for the Head and Neck case, using five gantry angles at couch=0° (0°, 72°, 144°, 216°, and 288°) as well as five gantry angles at couch=20° (180°, 220°, 260°, 300°, 340°).

Discussion

We provide four datasets for radiotherapy treatment plan optimization. The datasets are meant to serve several purposes:

- We provide datasets for reasearchers in the optimization community who may not have access to patient data.
- Advanced problems like BAO, DAO, and VMAT represent non-convex or combinatorial problems which typically cannot be solved to optimality. Thus, solution approaches are heuristics, and different methods can only be compared meaningfully based on common datasets, where differences due to patient geometry and dose calculation are eliminated.
- The datasets can serve as benchmark cases for the development of fast and efficient solvers customized to fluence map optimization and its variants. This development may also benefit other radiotherapy planning problems such as robust optimization in proton therapy and adaptive replanning in online image guided radiotherapy. Our datasets do not per se support these specific problems. However, such applications rely on very fast optimization methods that can handle large data.

Solution reporting

We recommend that researchers share results in the maximally transparent and reproducible manner. This includes the statement of the full optimization problem

that was solved. In addition, the solution should be shared in the form of fluence maps, from which the dose distribution and all dose measures can be derived. The details of the solution reporting may depend on the application:

- For IMRT fluence map optimization, the solution is the vector of beamlet intensities x at each beam (gantry/couch pair) that is used in the solution. As such, we recommend the following file format for users to report and share solutions. The file name should match the name of the Dij file (replacing the "_D.mat" with "_beamletSol.mat"), and should consist of fluence values stored as a vector called beamx. The beamlet solution files for the linear programs solved above are included in the data download.
- For DAO applications, the solution can be reported through an effective fluence map for each individual aperture, using the same format. Similarly, VMAT algorithms that represent extensions of DAO algorithms can report the solution in the form of effective fluence maps for all control points.

Fluence map optimization

We have presented results for the ones solutions and for simple linear programs for the purpose of data testing and consistency. We have not included solution times since the purpose of this paper is not to present methods for fast/quality solutions to the IMRT problem, but rather to provide a set of data for the community to do such things. We used the Matlab linear programming solver (linprog) to solve the TG119, the prostate, and the liver case, but switched to CPLEX's Matlab interface (cplexlp) to solve the head and neck case, due to its size. All cases finished in under two minutes, except for the head and neck case which took about 8 minutes.

The optimization formulation given in formulation 1 involves a linear mapping from the fluence values x to the voxel doses d. As such, provided the function $f(d)$ is convex and the constraint set C is convex, the problem is a convex optimization problem. Real world constraints often make the problem non-convex however (a non-convex objective would as well, although that seems less fundamental: there is no work that proves that non-convex objective functions are needed to produce high quality treatment plans). The discrete form of the beam angle optimization problem, where candidate beams are pre-selected and the optimization problem is to find a subset of the beams (for example, the seven best beams) and their beamlet fluences to optimize a given objective, is a combinatorial problem.

DAO and VMAT applications

In modern clinical treatment planning systems, fluence based optimization is done (at most) as an initial step. Final plan optimization involves determining aperture shapes (specified by the positions of MLC leaves) and weights. To than end, many modern planning systems apply DAO methods. Once a segment shape is computed, the dose is linear in the segment weight. To a first approximation, the dose contribution from a segment is the sum of the contributions from the individual beamlets that constitute that segment, i.e. the information stored in the D_{ij} matrix. But better accuracy is obtained by doing a dose computation for each individual aperture shape, which involves scatter terms that can only be computed once the aperture shape is known. Using the datasets provided herein, dose calculation for an aperture is limited to approximations based on the D_{ij} matrix. Despite this limitation,

this dataset can be used for DAO algorithm design. Indeed, most DAO algorithms heavily utilize the D_{ij} matrix concept for generating promising apertures [22] or for approximating gradients with respect to MLC leaf positions [27, 20]. Only a more accurate final or intermittent recalculation of an aperture's dose distribution cannot be performed using this dataset.

Similarly, VMAT treatments need to consider MLC leaf positions in order to emulate a clinical VMAT optimizer. VMAT solvers typically strive to find a solution where the beam rotates completely around the patient on the order of minutes. As such, complete fluence modulation cannot be achieved at every angle, and MLC leaf positions must be tracked to make sure neighboring apertures are similar so that the gantry does not need to slow down excessively to move the leaves far across the treatment field. Because this dataset involves beamlet position information and couch and gantry positions, it can be used for VMAT optimization research. To include delivery time in VMAT planning optimization one must specify a dose rate. A typical value is 600 MU/min.

Conclusion

We provide the first open dataset to the radiation oncology community, thus allowing researchers to compare methods for optimizing radiation dose delivery. The dataset comprises four patient cases from different sites. Besides CT data and structure sets, we also include dose calculation data in order to enable a one-to-one comparison of novel and existing optimization strategies for intensity modulated radiation therapy, beam angle optimization, direct aperture optimization, and volumetric-modulated arc therapy.

Appendix A: Coordinate systems

Figure 2 shows the conversion from voxel indices to voxel locations inside the patient. All patients in the data set are in standard orientation, i.e. supine and head first. The voxel with index "1" is located most anterior, superior, and to the patient's right. For voxel indexing, the anterior-posterior direction corresponds to the fastest changing index; the superior-inferior direction corresponds to the slowest changing index.

Figure 3(a) shows the definition of the beamlet grid. Throughout the dataset we assume a collimator angle of 0. For a couch angle of 0, the y-axis of the beamlet grid corresponds to the superior-inferior direction of the patient. For a gantry angle of 0, the x-axis of the beamlet grid corresponds to the left-right direction of the patient. Figure 3(b) shows the definition of the positive gantry and couch angles.

Appendix B: Demonstration code

For reading data into Python, the scipy package is used, and then the Matlab .mat files can be read directly. For example:

```
import scipy.io as io

beamDFile = io.loadmat('Gantry0_Couch0_D.mat')
```

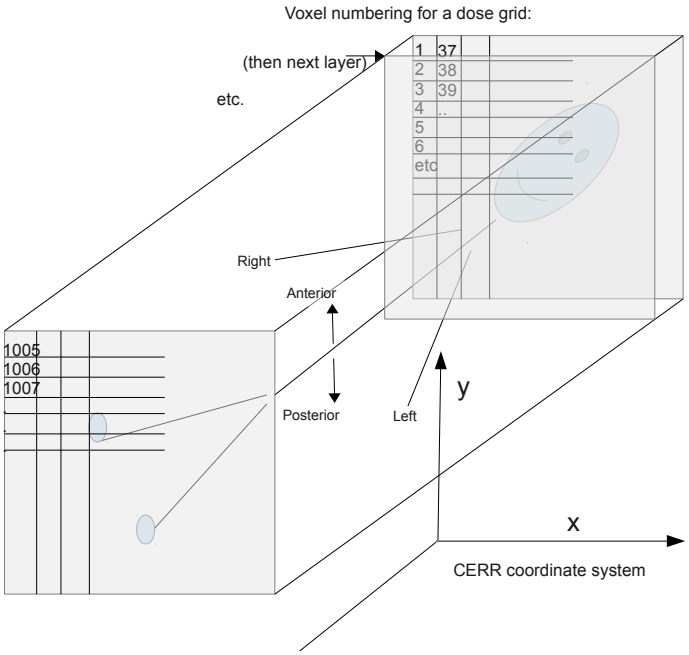

Figure 2 Voxel numbering A picture describing the voxel numbering pattern, the patient orientation, and the CERR coordinate system.

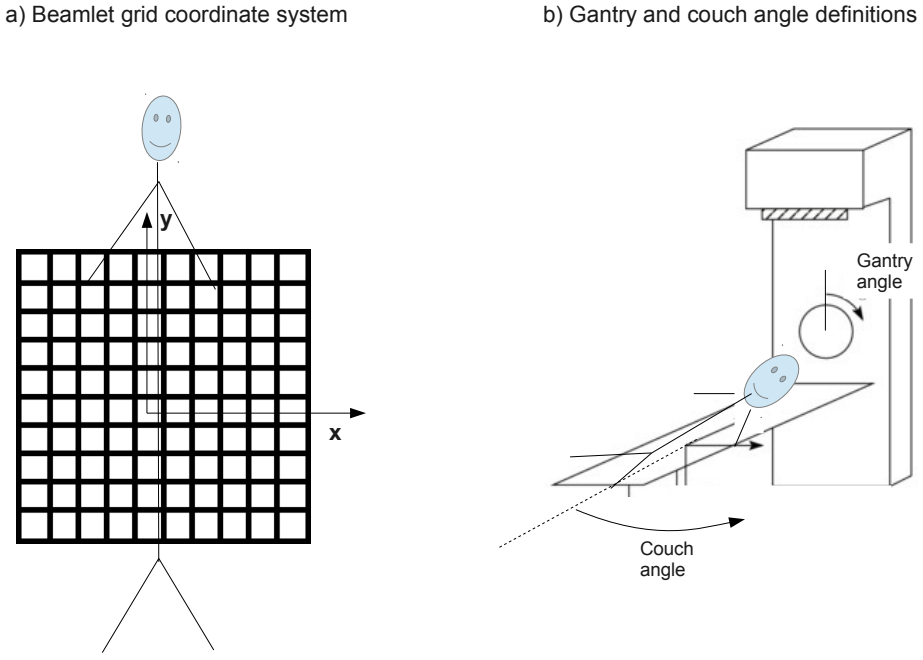

Figure 3 Beamlet grid, gantry angle, and couch angle definitions A picture displaying (a) the beamlet coordinate system used, for a sample beam placed at gantry angle 0 and couch angle 0, and (b) the definitions of the gantry and the couch angle.

```
dij = beamDFile['D']
```

Next we include two sample code snippets to assist people in getting started with the datasets in the Matlab environment. First we give a code which computes the mean dose to a structure for the ones solution of all of the beams in the current working directory.

```
beamdir = './';
allFiles = dir([beamdir '*D.mat']);
allNames = { allFiles.name };

d = [];

for i=1:length(allNames)
  f = allNames{i};
  %load the matrix D for the gantry/couch pair
  %stored in the file f:
  load(f)
  [nv, nb]=size(D);

  if i==1
    d = D*ones(nb,1);
  else
    d = d + D*ones(nb,1);
  end

end

fname = 'OuterTarget_VOILIST.mat';
%load a vector v of the voxel indices:
load(fname)

%get dose distribution for just those voxels:
dstruct = d(v);
%compute and display dose stats
dmin = min(dstruct);
dmean = mean(dstruct);
dmax = max(dstruct);
disp(['min, mean, max = ' num2str(dmin) ', ' ...
     num2str(dmean) ', ' num2str(dmax)]);
```

Next we give the code for obtaining a simple linear programming solution for the liver case. The first section of the matlab code reads the dose-influence matrix for 7 selected beam angles and constructs the concatenated D_{ij} matrix. Subsequently, the voxel lists for 5 of the structures are imported.

```
%Gantry and couch angles to use:
ga = [58 106 212 328 216 226 296];
```

```
ca = [0 0 0 0 32 -13 17];

Dij = 0;

%Form the Dij matrix
for i=1:length(ga)

    fname = ['Gantry' num2str(ga(i)) '_Couch' num2str(ca(i)) '_D.mat'];
    load(fname)

    %number of  beamlets at angle i
    nba(i) = size(D,2);

    if i==1
        Dij = D;
    else
        Dij = [Dij D];
    end

end

%Load structures
load('PTV_VOILIST.mat');
V{1} = v;
load('Liver_VOILIST.mat');
V{2} = v;
load('Heart_VOILIST.mat');
V{3} = v;
load('entrance_VOILIST.mat');
V{4} = v;
load('Skin_VOILIST.mat');
V{5} = v;
```

The next code section constructs a linear optimization problem as described in section . A weighted sum of the mean doses to the liver, the heart, and the normal tissue in the entrance region is minimized, subject to the constraints that every PTV voxel receives a dose larger than one. The linear program is solved using Matlab's build-in solver linprog. The optimal fluence map is returned into the vector x.

```
% mean doses contributions of all beamlets
Dlivermean = mean(Dij(V{2},:));
Dheartmean = mean(Dij(V{3},:));
Dentrancemean = mean(Dij(V{4},:));

%construct the linear inequality constraints
%to enforce a minimum dose of 1 to the PTV
A = -Dij(V{1},:);
```

```
b = -1*ones(size(A,1),1);

%cost vector
c = Dlivermean + Dheartmean + 0.6*Dentrancemean;

%bounds in beamlet intensity
nb = size(Dij,2); % total number of beamlets
lb = zeros(nb,1); % lower bound of zero
ub = 25*ones(nb,1); % upper bound of 25 MU

%optimization options
opt = optimset('Display','iter');
opt.LargeScale = 'on';

%solve problem using matlab's LP solver
[x, fval, eflag] = linprog(c,A,b,[],[],lb,ub,[],opt);
```

Next, the solution to the fluence map optimization problem is saved in the recommended format:

```
%save solution in our recommended format
ctr = 1;
for i=1:length(ga)
    fname = ['Gantry' num2str(ga(i)) '_Couch' ...
        num2str(ca(i)) '_beamletSol.mat'];
    %num beamlets at angle i = nba(i)
    beamx = x(ctr:ctr+nba(i)-1);
    save(fname,'beamx');
    ctr = ctr+nba(i);
end
```

Finally, the mean doses are reported and the 3D dose distribution is visualized. The vector of dose values is obtained by multiplying the dose influence matrix with the beamlet intensity vector. The dose vector is then converted into a 3D dose distribution based on the voxel numbering pattern described in appendix A. The voxel lists for the structures are converted to 3D binary masks and plotted as contours on top of the colorwash dose display. CERR users can use the CERR function showIMDose.

```
%report mean doses to structs:
Dlivermean*x
Dheartmean*x
Dentrancemean*x

%calculate dose distribution
d = Dij*x;

%reshape dose vector to 3-dimensional array
```

```
%dose grid dimensions
dim = [217 217 168];
%total number of voxels
nVoxels = 217*217*168;
%reshape dose vector
dose = reshape(d,dim);

%create 3-dimensional masks for structures
for(s=1:length(V))
    mask{s} = zeros(nVoxels,1);
    for(i=1:length(V{s}))
        mask{s}(V{s}(i))=1;
    end
    mask{s} = reshape(mask{s},dim);
end

%select axial slice to plot
slice = 50;

%plot dose and structures
figure;
set(gca,'DataAspectRatio',[1 1 1]);
set(gca,'YDir','rev');
axis([30 190 40 160]);
hold on;
%plot colorwash dose
imagesc(dose(:,:,slice));
%plot contours for PTV, Liver, Skin
for(s=[1 2 5])
    contour(mask{s}(:,:,slice),[0.5],'k','LineWidth',2);
end
hold off;
```

Competing interests
The authors declare that they have no competing interests.

Authors' contributions
DC carried out the overall project concept, the data generation, and the writing. DP modified CERR to be able to compute noncoplanar beams, and also tested the datasets. TL, MB and JU contributed to writing the manuscript and testing the datasets. Everyone proofread the manuscript.

Author details
[1]Massachusetts General Hospital, Harvard Medical School, Boston, MA. [2]German Cancer Research Center (DKFZ), Heidelberg, Germany. [3]University of Michigan, Ann Arbor, Michigan.

References

1. Alber, M., Nusslin, F.: Intensity modulated photon beams subject to a minimal surface constraint. Physics in Medicine and Biology **45**, 49–52 (2000)
2. Oelfke, U., Bortfeld, T.: Inverse planning for photon and proton beams. Med. Dosim. **26**, 113–124 (2001)
3. Webb, S.: A simple method to control aspects of fluence modulation in IMRT planning. Physics in Medicine and Biology **46**, 187–195 (2001)

4. Bangert, M., Ziegenhein, P., Oelfke, U.: Characterizing the combinatorial beam angle selection problem. Physics in Medicine and Biology **57**(20), 6707 (2012)
5. Wang, X., Zhang, X., Dong, L., Liu, H., Wu, Q., R., M.: Development of methods for beam angle optimization for IMRT using an accelerated exhaustive search strategy. Int. J. Radiation Oncology Biol. Phys. **60**(4), 1325–37 (2004)
6. Craft, D.: Local beam angle optimization with linear programming and gradient search. Physics in Medicine and Biology **52**(7), 127–135 (2007)
7. Breedveld, S., Storchi, P., Voet, P., Heijmen, B.: iCycle: integrated, multicriterial beam angle, and profile optimization for generation of coplanar and noncoplanar IMRT plans. Medical Physics **39**, 951 (2012)
8. Yu, C., Tang, G.: Intensity-modulated arc therapy: principles, technologies and clinical implementation. Physics in Medicine and Biology **56**(5), 31–54 (2011)
9. Craft, D., McQuaid, D., Wala, J., Chen, W., Salari, E., Bortfeld, T.: Multicriteria VMAT optimization. Medical Physics **39**, 686 (2012)
10. Bokrantz, R.: Multicriteria optimization for volumetric-modulated arc therapy by decomposition into a fluence-based relaxation and a segment weight-based restriction. Medical Physics **39**, 6712 (2012)
11. Papp, D., Unkelbach, J.: Direct leaf trajectory optimization for volumetric modulated arc therapy planning with sliding window delivery. Submitted **53**(4), 985–998 (2013)
12. Otto, K.: Volumetric modulated arc therapy: IMRT in a single gantry arc. Medical physics **35**, 310 (2008)
13. Bzdusek, K., Friberger, H., Eriksson, K., Hårdemark, B., Robinson, D., Kaus, M.: Development and evaluation of an efficient approach to volumetric arc therapy planning. Medical physics **36**, 2328 (2009)
14. Meng, B., Zhu, L., Widrow, B., Boyd, S., Xing, L.: A unified framework for 3D radiation therapy and IMRT planning: plan optimization in the beamlet domain by constraining or regularizing the fluence map variations. Physics in Medicine and Biology **55**(22), 521 (2010)
15. Khan, F., Craft, D.: 3d conformal planning using low segment multi-criteria imrt optimization. arXiv **100**(100), 100 (2014)
16. Yarmand, H., Winey, B., Craft, D.: Guaranteed epsilon-optimal treatment plans with the minimum number of beams for stereotactic body radiation therapy. Physics in Medicine and Biology **58**(17), 5931 (2013)
17. Salari, E., Unkelbach, J.: A column-generation-based method for multi-criteria direct aperture optimization. Physics in Medicine and Biology **58**(3), 621 (2013)
18. Shepard, D., Earl, M., Li, X., Naqvi, S., Yu, C.: Direct aperture optimization: A turnkey solution for step-and-shoot IMRT. Medical Physics **29**, 1007–1018 (2002)
19. Men, C., Romeijn, H., Taşkın, Z., Dempsey, J.: An exact approach to direct aperture optimization in IMRT treatment planning. Physics in Medicine and Biology **52**, 7333 (2007)
20. Cassioli, A., Unkelbach, J.: Aperture shape optimization for IMRT treatment planning. Physics in Medicine and Biology **58**(2), 301 (2013)
21. Carlsson, F.: Combining segment generation with direct step-and-shoot optimization in intensity-modulated radiation therapy. Medical physics **35**, 3828 (2008)
22. Romeijn, H.E., Ahuja, R.K., Dempsey, J.F., Kumar, A.: A column generation approach to radiation therapy treatment planning using aperture modulation. SIAM Journal on Optimization **15**(3), 838–862 (2005)
23. Deasy, J., Blanco, A., Clark, V.: Cerr: A computational environment for radiotherapy research. Medical Physics **30**(5), 979–985 (2003)
24. Kalinin, E., Deasy, J.: A method for fast 3-D IMRT dose calculations: The quadrant infinite beam (QIB) algorithm. In: Medical Physics, vol. 30, pp. 1348–1349 (2003)
25. Ezzell, G., Burmeister, J., Dogan, N., LoSasso, T., Mechalakos, J., Mihailidis, D., Molineu, A., Palta, J., Ramsey, C., Salter, B.e.a.: IMRT commissioning: multiple institution planning and dosimetry comparisons, a report from AAPM Task Group 119. Medical Physics **36**(11), 5359–5373 (2009)
26. Jelen, U., Sohn, M., Alber, M.: A finite size pencil beam for IMRT dose optimization. Physics in Medicine and Biology **50**(8), 1747–1766 (2005)
27. Hårdemark, B., Liander, A., Rehbinder, H., Löf, J.: Direct machine parameter optimization with RayMachine® in Pinnacle3®. RaySearch White Paper. Stockholm, Sweden: RaySearch Laboratories AB (2003)

Figures

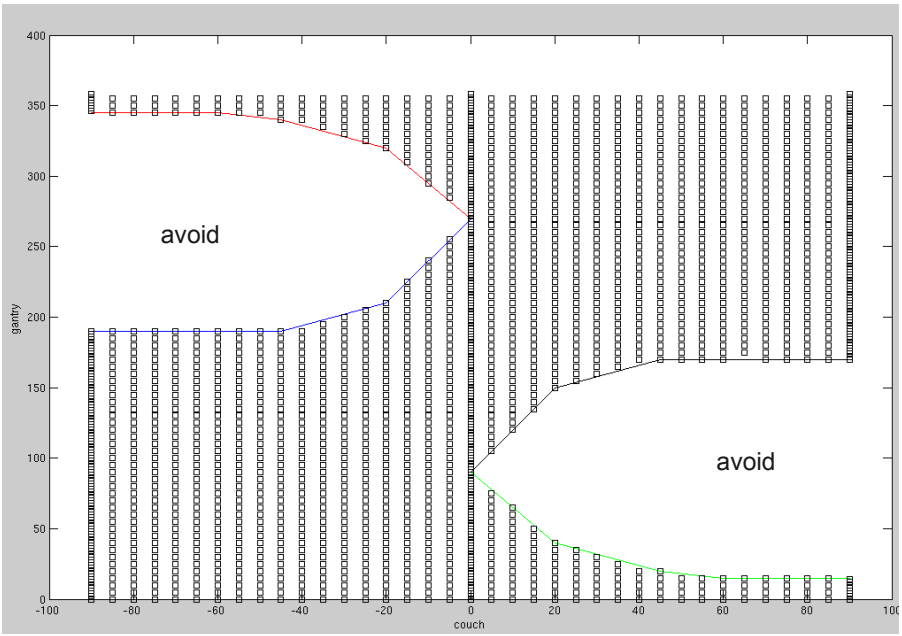

Figure 4 Elimination map for head and neck angles A picture displaying the couch/gantry angle pairs that were eliminated due to the beam entering the inferior CT slice, thus causing an incorrect dose computation.